J. Membrane Biol. 15, 363–382 (1974)

Dimensions of Polar Pathways Through Rabbit Gallbladder Epithelium

The Effect of Phloretin on Nonelectrolyte Permeability

C. H. van Os, M. D. de Jong and J. F. G. Slegers

Department of Physiology, University of Nijmegen, Nijmegen, The Netherlands

Received 9 July 1973; revised 29 October 1973

Summary. The permeability of rabbit gallbladder to hydrophilic nonelectrolytes, with molecular weights from 20 to 60,000, has been studied. Restriction in the diffusion of the small electrolytes is very significant up to glycerol, which suggests permeation through aqueous pores with equivalent radii of 4 Å. An extracellular pathway is responsible for the permeation of the larger solutes. This extracellular pathway shows no restriction in diffusion of molecules up to the size of inulin. Dextran (15,000 to 17,000 mol wt) is significantly restricted. Albumin permeability is $<10^{-8}$ cm sec^{-1}. These observations can be equated with equivalent pore radii of $\sim$40 Å for the shunt pathway.

Increasing osmolarities of the incubation medium cause decreased cell-membrane permeability and increased shunt permeability. 0.5 mM phloretin induces a 60% reduction in urea permeability and a 168% increase in antipyrine permeability. No effect on the osmotic water permeability or on the shunt permeability is observed in the presence of phloretin. The apparent activation energy of urea permeation changes from values consistent with diffusion in bulk water, to values consistent with diffusion through hydrocarbon regions. This suggests that the polar route for urea permeation is blocked by phloretin.

The contribution of the shunt pathway to osmotic flow induced by sucrose or NaCl gradients is smaller than 16% according to Poiseuille's flow calculations. Tetraethylammoniumchloride and albumin have been shown to be osmotically more effective than sucrose, suggesting a greater shunt contribution to the total water flow.

Extensive studies on nonelectrolyte permeability of rabbit gallbladder epithelium have led to the postulation of small aqueous pores in the cell membranes and a small number of larger pores somewhere in the epithelium [13, 48, 56]. In this respect gallbladder epithelium resembles the epithelium of kidney proximal tubules [5, 23], stomach [1] and small intestine [33]. In all these tissues the anomalous permeability of relatively large hydrophilic solutes, such as sucrose, inulin and even bigger molecules, is explained by postulating the existence of some large aqueous pores in the epithelium.

The tissues mentioned share another feature in common. Recently, electrophysiological investigation has provided evidence for an extracellular shunt pathway for ions in proximal tubules [7], stomach [6], small intestine [21], and in gallbladder [2, 22]. In *Necturus* gallbladder the shunt route has been demonstrated to lead through the junctional complexes [22].

It is attractive to correlate the anomalous nonelectrolyte permeability of these epithelia with the extra-cellular shunt pathway for passive ion permeation. In this case the permeation of solutes through the shunt pathway must be limited by the morphological dimensions of the tight junctions, i.e. the zonulae occludentes. Therefore, we studied the permeation of a series of hydrophilic solutes with molecular weights ranging from 60 to 60,000. The results suggest two polar pathways through the epithelium, one with an equivalent radius of approximately 4 Å and another with a radius of about 40 Å.

Independent pathways for water and small nonelectrolytes could be demonstrated in the membranes of the red cell [37, 40] and the toad bladder [20] by treating the membranes with phloretin. Since these observations seriously undermine the small aqueous pore hypothesis, we studied the effect of phloretin on gallbladder nonelectrolyte permeability.

Materials and Methods

Tissue Preparation

Gallbladders are obtained from albino rabbits of both sexes by dissection. Cannulation of bladders and removal of bile has been described previously [53]. Sac preparations of cannulated gallbladders are suspended in Ringer's solutions, the temperature of which is controlled within 0.5 °C. The serosal side of the bladder faces the outer bathing solution. The luminal side can be reached through a cannula. Ringer's solutions of the following composition are used: (mM) NaCl, 145; KCl, 5.0; $CaCl_2$, 1.0; $MgCl_2$, 1.0; NaH_2PO_4, 0.375; Na_2HPO_4, 2.125; pH, 7.4, osmolarity 288 mOsm × liter^{-1}. Solutions are continuously gassed with 100% O_2, water saturated.

Permeability Measurements

Osmotically induced water flows are measured gravimetrically as described by Diamond [12]. Osmotic water permeability P_f and diffusive permeabilities P_d are calculated as described previously and expressed in cm sec^{-1} [54]. The rate of diffusion of nonelectrolytes is determined as follows: The bladder is suspended in 10 ml Ringer's solution stirred by O_2 bubbles and a magnetic flea. ^{14}C-labeled specimens of *n*-butanol, urea, ethylene glycol, glycerol, erythritol, mannitol, sucrose, inulin, antipyrine, dextran (15,000 to 17,000 mol wt) or ^{125}I-labeled bovine serum albumin (BSA) are added to the luminal solution in separate experiments. After applying the isotope, the luminal content is sucked several times into the syringe, but during the flux measurement the luminal

solution is effectively unstirred. The bladder makes gentle regular movements induced by the magnetic stirrer in the serosal solution. The amount of radioactivity of ^{14}C-labels used ranges from 1.0 μC to 2.5 μC, and 50 μC ^{125}I is used in experiments with albumin.

According to the solute size, time intervals and volume of samples taken from the serosal solution are varied. After each sample is withdrawn the volume of the serosal solution is restored by adding an equal amount of cold Ringer's solution. Corrections for dilution are made for sample sizes $\geqq 50$ μliters.

The rate of appearance of butanol, urea and antipyrine in the serosal solution decreases exponentially with time. This is probably due to high fluxes which lead to the dissipation of the isotope gradients across the tissue [48]. Therefore, the permeabilities of these solutes are calculated from extrapolated zero time fluxes as described previously [54]. All other solutes show a linear behavior over the time period of flux measurements, which varies from 20 to 150 min. Determination of gallbladder volume, surface area and initial isotope concentration in the luminal solution has been previously described [54].

^{125}I-bovine serum albumin is passed over Sephadex G-25 immediately before use in order to remove free ^{125}I-label. The albumin fraction is made isotonic with NaCl and the albumin concentration is brought to 6% by adding cold BSA. Samples of 1 ml are taken from the serosal solution every 15 min. Dextran (15,000 to 17,000 mol wt) is passed over Sephadex G-25, but filtered samples behave indistinguishably from unfiltrated specimens. The other radioactive tracers were not examined for purity. The radioactive counts that emerged into the serosal solution have not been tested by radiochromatography. ^{14}C-isotope samples are counted in a Packard liquid scintillation counter (Model 314E) using Bray's [9] cocktail. ^{125}I-samples are counted in glass vials in a Philips λ-counter (Model PW-4003/4251). Dextran-carboxyl-^{14}C (15,000 to 17,000 mol wt), Antipyrine-N-methyl-^{14}C and ^{125}I-bovine serum albumin are obtained from NEN chemicals GmbH, W.Germany. All other ^{14}C-labeled solutes are obtained from the Radio Chemical Centre, Amersham, England.

Unstirred Layer Corrections

Unstirred water layers adjacent to membranes cause, in general, considerable underestimation of diffusive permeabilities, especially of relatively fast permeating substances. In rabbit gallbladder, diffusion of *n*-butanol has been proven to be completely unstirred-layer limited [48, 54]. Therefore, observed diffusive permeabilities are corrected for unstirred-layer influences by using "unstirred-layer thickness", determined from butanol diffusion and free solution diffusivities of the solutes listed in Table 1. Corrections are calculated with an equation for resistances in series as described previously [54]; i.e., $\frac{1}{P_{obs_i}} = \frac{1}{P_{true_i}} + \frac{\delta_{but}}{D_i}$, where P_{obs_i} = observed permeability for solute i, P_{true_i} = true permeability for solute i, D_i is free solution diffusivity, and $\delta_{but} = \frac{D_{butanol}}{P_{butanol}}$ = thickness of total unstirred layers. $D_{butanol}$ used for unstirred layer thickness calculation was taken from Lyons and Sandquist [36]. (1.0×10^{-5} cm^2 sec^{-1}).

Temperature, Osmolarity and Phloretin Effects

Temperature dependence of diffusive permeabilities is determined between 5 and 35 °C at intervals of 10 °C.

The influence of osmolarity on P_d values is studied in three media: Medium I: Ringer's solution diluted 1:1 with distilled water (155 mOsm × liter^{-1}); Medium II:

Table 1. Solute properties of tracer substances used

Solute	mol wt	$D_{calcul.}$ D_{ref} 10^{-6} cm^2 sec^{-1} (25°)			Molecular radii (Å)	
^{3}HHO	20	22.2	23.6	[55]	1.5	[24]
Urea	60	12.8	13.8	[34]	2.4×2.9	[49]
Ethylene glycol	62	12.6	—		2.4×3.5	[49]
Glycerol	92	10.3	—		3.0×3.9	[49]
Erythritol	122	9.0	—		3.5×4.2	[49]
Mannitol	182	7.4	6.7	[34]	4.3	[46]
Sucrose	364	5.2	5.2	[34]	5.2	[46]
Inulin	$5\cdot10^3$	1.7	1.6	[28]	6×50	[41]
Dextran	$15-17\cdot10^3$	1.15	—		14×100	[5, 39]
Albumin	$60\cdot10^3$	0.74	0.66	[35]	37	[17]

Free solution diffusivities are calculated from the relationship: $DM^{\frac{1}{3}} \sim$ constant for $30 \leqq M \leqq 360$ and $DM^{\frac{1}{3}} \sim$ constant for mol wt $\geqq 360$ using $D_{sucrose} = 5.2 \times 10^{-6}$ cm^2 sec^{-1} as reference [50]. Calculated values agree well with values from the literature. The small molecules are treated as cylinders [49]. The dimensions given represent the radius and half the length of the cylinder. The dimension of dextran, 15 to 17×10^3, is calculated from the dimension of dextran 60 to 90×10^3 given by Bentzel *et al.* [5], assuming the same ellipticity factor for both molecules, and volumes proportional to their molecular weights [39].

Medium I plus 200 mmoles × liter^{-1} sucrose, (370 mOsm × liter^{-1}); Medium III: Medium I plus 400 mmoles × liter^{-1} sucrose, (620 mOsm × liter^{-1}). Osmolarity influence on osmotic water permeability P_f is also determined in media I, II and III with an additional 100 mOsm × liter^{-1} sucrose in the serosal solution. The osmolarity of the solutions is measured by freezing point depression determination with an Advanced osmometer (Advanced Instruments Inc.). The viscosity increase in the solutions caused by adding sucrose is measured with an Ubbelohde viscosity meter. This viscosity increase is taken into account in unstirred layer corrections of diffusive permeabilities.

Phloretin is dissolved in ethanol 96%. Ringer's solutions are brought to 0.5 mM phloretin and 0.5% ethanol. The lumen of the bladder is filled with this solution. The effect on the permeability is tested after 75 min of incubation with phloretin. The control values are measured with 0.5% ethanol in the mucosal solution since ethanol alone caused a small increase in urea permeability in three control bladders.

Results

Diffusive permeabilities $P_{d(i)}$ have been determined for the solutes whose properties are listed in Table 1. All these solutes have low ether/water partition coefficients. A typical result from a ^{125}I-albumin flux experiment is given in Fig. 1.

During the first 45 min small amounts of radioactivity appear in the serosal solution, but this activity remains constant during the following

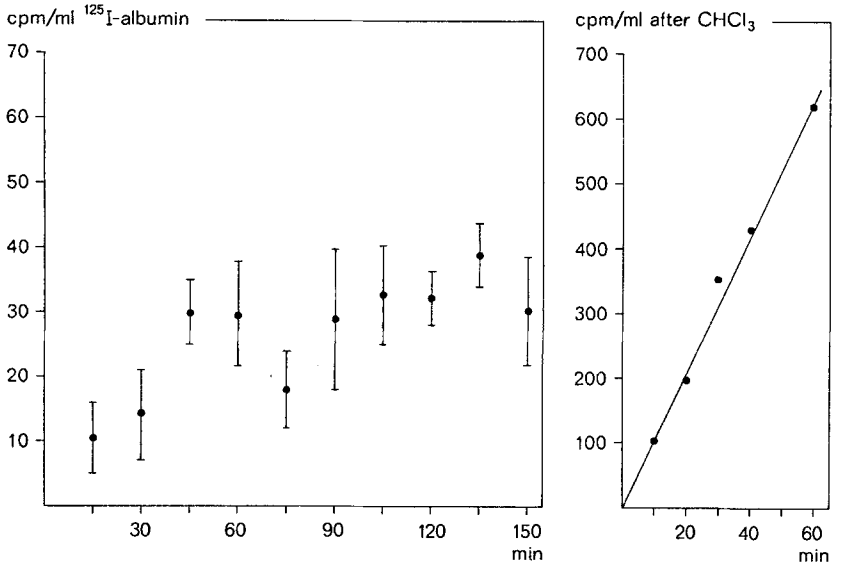

Fig. 1. *Left*: typical example of ^{125}I-albumin flux through gallbladder epithelium. The points represent mean values plus SD of five countings. *Right*: ^{125}I-albumin flux through the same bladder after 10 min $CHCl_3$ exposure

Table 2. Comparison of albumin and inulin permeabilities in seven gallbladders

P_{inulin} (P_d in 10^{-6} cm sec^{-1})	$P_{albumin}$	$P_{albumin\ after\ CHCl_3}$	$P_{inulin}/P_{albumin}$ ($D_{inulin}/D_{albumin}=2.7$)
15.0	0.23	—	65
0.99	<0.01	—	< 99
5.1	0.02	—	232
2.2	<0.01	1.62	<220
13.5	0.17	1.50	79
4.5	<0.01	—	<450
3.1	<0.01	—	<310

In two bladders, albumin permeation is measured after $CHCl_3$ treatment of the epithelium. $P_{albumin} < 0.01 \times 10^{-6}$ cm sec^{-1} cannot be observed with the method used.

2 hr despite the fact that the hot side contains 0.5×10^6 cpm/ml. Therefore, we conclude that small amounts of free ^{125}I-tracer equilibrate in the first 45 min and give rise to approximately 30 cpm/ml above the blank value of 250 cpm/ml in the serosal solution. The free tracer amount is less than 0.1 %, which is negligible.

Table 2 gives the result of albumin fluxes in seven gallbladders together with the inulin permeabilities. Observable albumin fluxes are accompanied

Table 3. Diffusive permeabilities of rabbit gallbladder epithelium

Solute	P in 10^{-6} cm sec^{-1}		Shunt pathway			Cell membrane
			Free solution	Restricted diffusion pore radius 40 Å		
	$P_{d(i)}$	n	$P_{S(i)}$	D_p/D_0	$P'_{s(i)}$	$P_{m(i)}$
^{3}HHO (ref. [54])	1590 ±290	(10)	33	0.82	49	1540±290
Urea	84 ±8	(35)	19	0.77	27	56±8
Ethylene glycol	34 ±6	(11)	18	0.77	25	9±6
Glycerol	24 ±5	(8)	15	0.71	19	5±5
Erythritol	15 ±4	(7)	13	0.67	15.8	–
Mannitol	9.7±2.8	(13)	10.6	0.62	11.8	–
Sucrose	7.6±1.4	(16)	7.6	0.55	7.6	–
Inulin	2.9±0.6	(37)	2.5	0.50	2.3	–
Dextran	1.02±0.26	(7)	1.68	0.23	0.70	–
Albumin	<0.01	(7)	0.96	0.005	0.0087	–

Observed permeabilities, corrected for unstirred layer effects as described in Materials and Methods are tabulated in the first column (number of observations in parentheses). Diffusive permeability of ^{3}HHO has been published previously [54]. Free solution shunt permeabilities are calculated from $P_{S(i)}=(D_i/D_{\text{sucrose}})P_{\text{sucrose}}$, where D_i and D_{sucrose} are free-solution diffusivities and P_{sucrose} is the observed sucrose permeability. Hindrance of diffusion in pores with $r=40$ Å is calculated from the Renkin equation [43]: $D_p/D_0=(1-\alpha)^2\times(1-2.104\,\alpha+2.09\,\alpha^3-0.95\,\alpha^5)$ where D_p/D_0 is the ratio of solute diffusivity in the pore to that in free solution, and $\alpha=R_s/R_p$ is the ratio of solute radius to pore radius. The smallest solute radius of Table 1 is used for calculating restriction in the diffusion. Shunt permeabilities, when restriction of diffusion is taken into account, are listed in the fourth column and are calculated from

$$P'_{s(i)}=\frac{(D_p/D_0)_i}{(D_p/D_0)_{\text{sucrose}}}\cdot P_{s(i)}.$$

Cell membrane permeabilities are calculated from $P_{m(i)}=P_{d(i)}-P'_{s(i)}$.

by inulin permeabilities five times the mean value given in Table 3. Bladders with inulin permeabilities near this mean value show apparent impermeability to albumin, which means $P_{\text{albumin}}<10^{-8}$ cm sec^{-1}, since $P<10^{-8}$ cannot be measured by this method at this tracer concentration. Apparent impermeability to albumin indicates that the size of the apertures through which inulin permeates is about the size of the albumin molecule. This implies that the permeation of sucrose and inulin through the gallbladder wall is not caused by "damaged" or "missing" cells. High inulin permeability accompanied by a detectable albumin flux is therefore considered to be the result of tissue damage.

In Table 3, diffusive permeability coefficients of various solutes, corrected for unstirred layer effects, are tabulated in the first column. The mean value of unstirred layer thickness, determined by butanol diffusion, is 837 ± 42 μ ($n = 32$), not significantly lower than values reported by Smulders and Wright [48] for similar epithelium. Since inulin and sucrose permeation are not due to damaged cells and since a great variety of plasma membranes studied so far are fairly impermeable to both solutes, we may postulate that these solutes are passing extracellularly.

Assuming a free solution shunt and using P_{sucrose} as a reference, then the shunt permeability for the other solutes can be calculated (Table 3, second column). The dimension of this shunt path is about the dimension of the albumin molecule, and assuming circular pores, the radii must be $\leqq 40$ Å.

Diffusion of the solutes used through pores of this size is significantly restricted [3]. This restricted diffusion is adequately described by the Renkin equation [43]. Table 3, third column, gives restricted diffusion values for the various solutes.

The free solution shunt values have been corrected for this restriction effect in the fourth column. The results of Table 3 suggest that diffusion of water and urea is predominantly through the cell membranes and not through the extracellular pathway for sucrose. The contribution of this shunt to an osmotic water flow will be dealt with in the Discussion. The permeability pattern of the small hydrophilic solutes is in agreement with the aqueous pore hypothesis. Phospholipid bilayers, doped with polyene antibiotics, and erythrocyte membranes exhibit an identical permeability pattern [24, 27]. This resemblance suggests permeation through pores with equivalent radii of about 4 Å. From erythritol to dextran, the permeation is exclusively through the shunt. The restriction in the diffusion of dextran and albumin is adequately described by diffusion through pores with radii of about 40 Å.

Smulders, Tormey and Wright [47] have shown that osmotically induced water fluxes through the gallbladder wall greatly influence the magnitude of other solute fluxes; a waterflux from lumen to serosa causes a $4\times$ greater solute flux than a waterflux in the opposite direction. This could be ascribed to morphological changes; i.e., the lateral intercellular spaces dilate or collapse under influence of the water flow.

To study osmolarity influences on permeability we have to work under zero water flow conditions. This was achieved by raising or lowering the osmolarity on both sides of the gallbladder wall and measuring solute

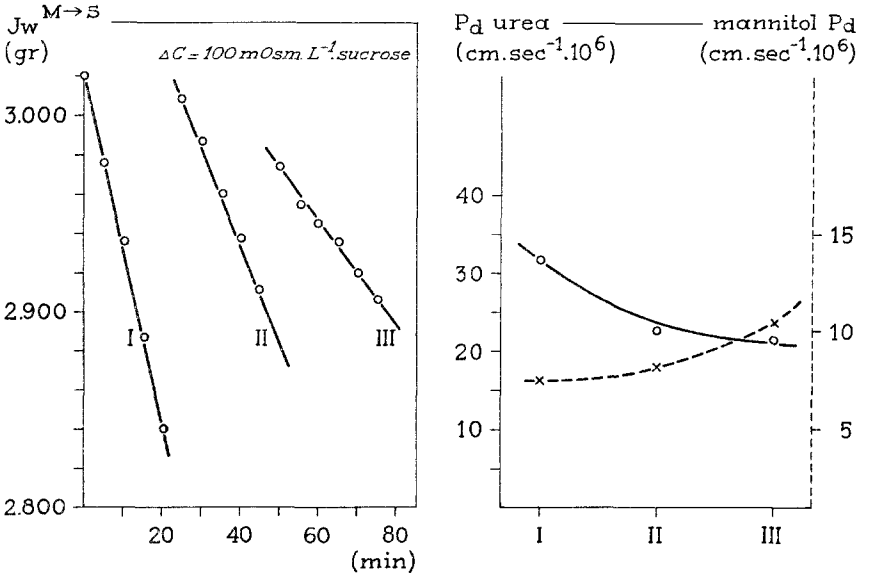

Fig. 2. Effect of medium osmolarity on osmotic water flow and urea and mannitol permeabilities. Medium I: 155 mOsm × liter^{-1}; II: 370 mOsm × liter^{-1}; III: 620 mOsm × liter^{-1}. The water flow is generated with 0.1 Osm × liter^{-1} sucrose in the serosal solution. Urea (left) and mannitol (right) fluxes were determined under zero volume flow conditions. The effect of different medium osmolarities on solute fluxes is determined in one gallbladder. Starting in medium III or in medium I gave the same results

fluxes at 10 °C. No net water fluxes could be observed under these conditions. An osmolarity increase reduces water and urea permeability but enhances the permeability to mannitol (Fig. 2). The relative increase or decrease in permeability in media I and III is given for several solutes in Fig. 3. The osmolarity effect indicates clearly the existence of different routes for the smaller and larger solutes.

The drastic effect of phloretin on the permeability to small hydrophilic solutes of red cell membranes, justifies a study on phloretin effects in gallbladder membranes to find out if this phenomenon is a more general one. Owen and Solomon [40] reported that phloretin affects hydrophilic as well as hydrophobic solute permeation and therefore we studied the effect of phloretin on water, urea, antipyrine and inulin permeability. The results are tabulated in Table 4. The osmotic water flow is not influenced by phloretin while the reduction in urea permeability is very marked. This result agrees with Macey and Farmer's [37] observation. Antipyrine permeability is increased as in the red cell [40]. The shunt pathway is not altered. Although

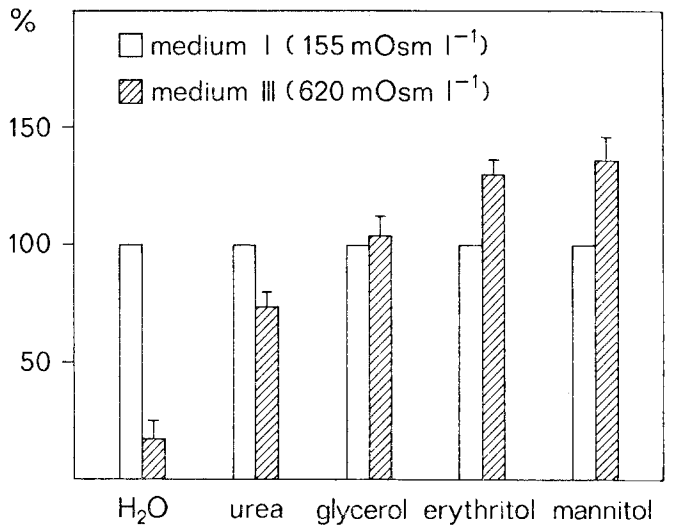

Fig. 3. Effect of medium osmolarity on nonelectrolyte permeability of gallbladder epithelium. The observed permeabilities in medium III have been normalized to control values determined in medium I (100%). Mean values of six determinations are given with SE values on top of the bars

Table 4. Effect of phloretin on nonelectrolyte permeabilities

	$P_{phloretin}/P_{control}$	$\frac{(P_{phloretin}-P_{shunt})}{(P_{control}-P_{shunt})}$
Water	0.97±0.04 (5)	–
Urea	0.54±0.08 (8)	0.39±0.05 (8)
Antipyrine	1.43±0.14 (6)	1.68±0.15 (6)
Inulin	0.99±0.02 (5)	–

The effect of 0.5 mM phloretin is expressed as the ratio of permeability coefficients with and without phloretin ($P_{phloretin}/P_{control}$). $P_{control}$ is measured with 0.5% ethanol added to the luminal Ringer's solution and $P_{phloretin}$ is measured in the same gallbladder. Mean values are given with SE and number of observations in parentheses. P values for urea and antipyrine are corrected for unstirred layer effects. Corrections of P values for shunt contributions are made on the basis of free solution diffusivities and observed inulin permeabilities. $P_{shunt}=(D_i/D_{inulin})\times P_{inulin}$.

the magnitude of the phloretin effect is somewhat smaller, the results are similar to those found in toad bladder and in red cell membranes.

Smulders and Wright [48] have shown that apparent activation energies of solute permeation in rabbit gallbladder suggest three pathways: the membrane lipid core, an aqueous extracellular route, and an aqueous route

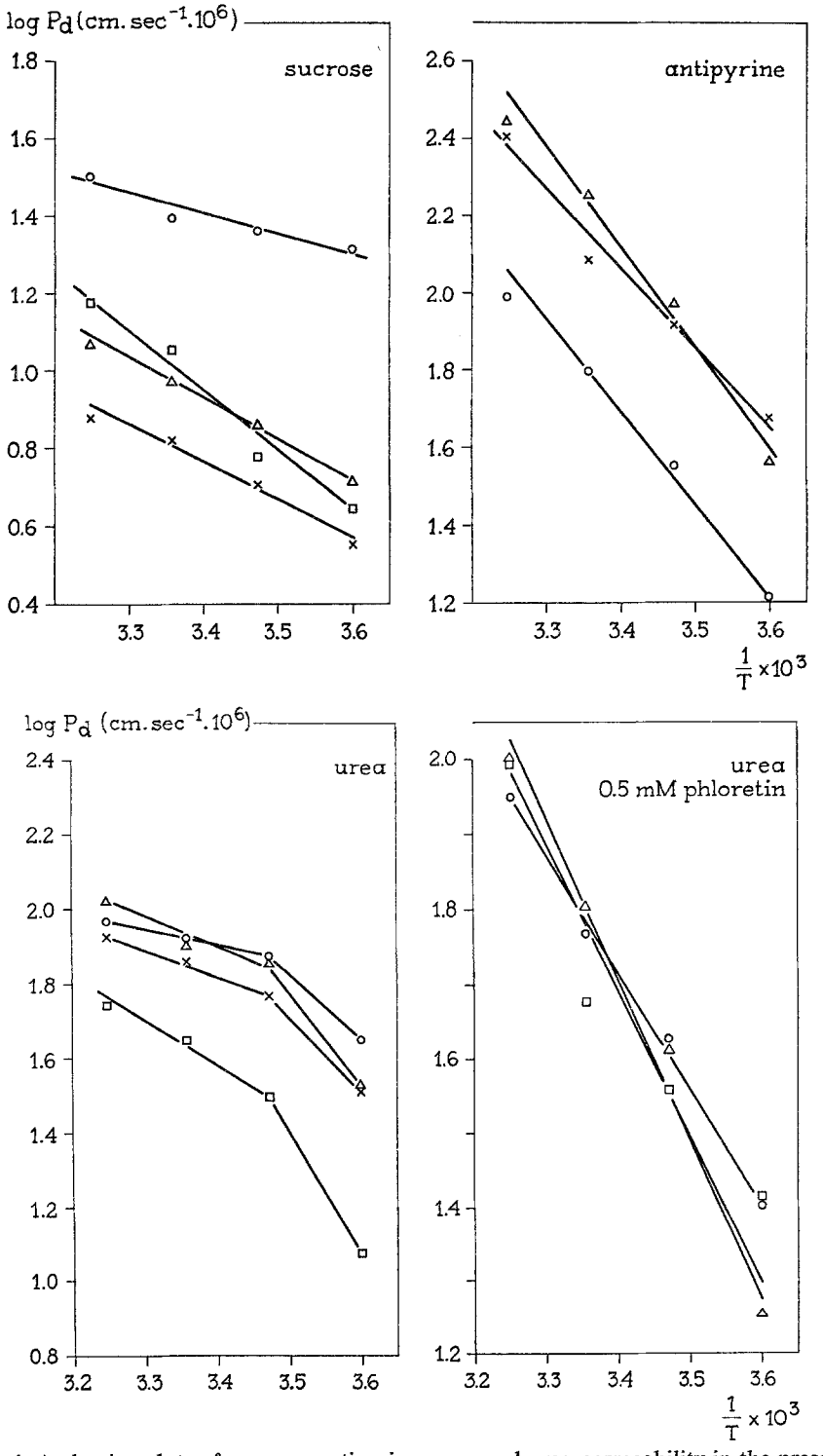

Fig. 4. Arrhenius plots of sucrose, antipyrine, urea and urea permeability in the presence of 0.5 mM phloretin. One line connects points observed in the same gallbladder. Apparent activation energies are calculated from the slopes $\times 4.575$ kcal $\times$ mole^{-1}

Table 5. Comparison of osmotic efficiency of equal osmotic gradients of several solutes

	Sucrose	NaCl	Na_2SO_4	TEACl	Albumin
$J_{V_i}/J_{V_{sucrose}}$	1.00	0.81±0.07	1.04±0.02	1.38±0.09	1.49±0.12
n		(5)	(5)	(7)	(9)

Water fluxes induced by 100 mOsm × liter^{-1} gradients of NaCl, Na_2SO_4 and TEACl are directly compared with fluxes induced by sucrose in the same gallbladder. Water fluxes induced by 20% albumin Ringer's solution (~20 mOsm liter^{-1}) are compared with 20 mOsm × liter^{-1} sucrose, since the medium osmolarity has a drastic effect on P_f (Fig. 2). The results are normalized to the sucrose-induced water fluxes, $(J_{V_i}/J_{V_{sucrose}})$, and given with SE values. $\bar{J}_{V_{sucrose}}(M \rightarrow S) = 32.4 \pm 4.8$ (10) μliter × hr^{-1} cm^{-2}.

through the membranes. We studied the effect of temperature on urea, antipyrine and sucrose permeation and on urea and antipyrine permeation in the presence of phloretin.

The Arrhenius plots of urea (Fig. 4) are similar to the Arrhenius plots of osmotic water permeability published previously [54]. This again suggests the same route for water and urea through the membranes. The mean value for the apparent activation energy of urea is below 15 °C: 10.1 kcal × mole^{-1} and above the transition phase 3.5 kcal × mole^{-1}. Phase transitions do not occur in sucrose and antipyrine plots. Mean values for activation energies are 5.2 and 10.5 kcal × mole^{-1} for sucrose and antipyrine, respectively. Phloretin changes the Arrhenius plot of urea completely. The phase transitions disappear and the activation energy is shifted to a mean value of 9.6 kcal × mole^{-1}. This suggests that phloretin blocks the aqueous pathway for urea and that permeation is only possible via the membrane lipid core. No effect of phloretin on the activation energy of antipyrine permeation could be observed. To evaluate the shunt contribution to osmotic flow, we compared osmotic water flows induced by NaCl, Na_2SO_4, tetraethylammoniumchloride (TEACl), and albumin gradients with sucrose-induced flows. Table 5 gives the results. TEACl and albumin are more effective than sucrose, while NaCl is a less effective osmotic agent. Assuming a reflection coefficient, $\sigma = 1$, for sucrose in the cell membrane, the increase in flow with TEACl and albumin must be due to flow through the extracellular shunt.

Discussion

Extensive studies on nonelectrolyte permeation through rabbit gallbladder epithelium have been carried out by Wright and Diamond [56] and Dia-

mond and Wright [13]. These authors made use of the fact that streaming potentials induced by osmotic gradients were directly proportional to the water flow rate. The results of the osmotic studies have been confirmed with radioactive tracer methods by Smulders and Wright [48]. For information about the relationships between chemical structure and permeability pattern we can refer to these studies.

Two aspects of nonelectrolyte permeability of rabbit gallbladder have led to the initiation of this investigation; i.e., the fast relative permeation of small polar solutes and the permeation of relatively large polar solutes such as sucrose and inulin.

We carried out our flux measurements with a sac preparation of the gallbladder and compared our results with the data of Smulders and Wright [48], obtained with an Ussing chamber technique. The permeability to inulin and sucrose is significantly greater in the sac preparation, while no differences are observed for the smaller solutes. Probably, in the natural configuration when the lumen is filled with fluid, the surface infoldings are less extensive than in a flat preparation, thus the shunt-path may be more stretched or better accessible. The advantages of the sac preparation over the Ussing chamber are a considerable gain in time for isotopic flux determinations, and edge damage effects which can be caused by clamping the tissue between the Lucite half-chambers, are avoided.

The permeability pattern of the small polar solutes (last column, Table 3) is in agreement with the small aqueous pore hypothesis. Soll [49] has shown that when the probing molecules are treated as cylinders, the restriction of diffusion through small pores correlates with the length of the cylinder. From Tables 1 and 3 it can be seen that P_m correlates better with the length than with the diameter of the molecules. The aqueous pore model, based on the violation by small polar solutes of Overton's rule, predicts passage of water and urea through the same pathway. Since the deviation from Overton's rule is very marked in erythrocytes and in rabbit gallbladder [26], and since phloretin dissociates the water and urea pathway in red cell membranes [37, 40] it is an interesting observation that phloretin brings about the same effect in gallbladder membranes. This dissociation between the movement of water and urea undermines the aqueous pore model severely. Owen and Solomon [40] ascribed the effect of phloretin on red cell membranes to specific interaction with a membrane protein. Conformational changes in this particular protein or protein complex, would affect the aqueous path for urea permeation as well as the permeation through the membrane lipid core as indicated by the increased antipyrine permeability.

The shift in apparent activation energy of urea, brought about by phloretin, strongly suggests a transition from an aqueous path to a more hydrophobic route, which supports Owen and Solomon's explanation. However, an inadequate unstirred layer correction could be responsible for the break in the Arrhenius plot of urea and the disappearance with phloretin. An underestimated unstirred layer causes a greater underestimate of the higher permeabilities at the higher temperature. There are three arguments against this explanation. First, if the phase transition for urea were an artifact of an underestimated unstirred layer correction, one would expect a similar bend in the Arrhenius plot for antipyrine, since this is a fast permeating solute too. The contribution of the unstirred layers to the total resistance to urea diffusion at 35 °C was 37% and in the case of antipyrine, 48%. The Arrhenius plots of antipyrine are straight, which is a strong argument in favor of a real phase transition in the urea plots. Second, if the plots of urea in Fig. 4 have to be straight, the P_{urea} values at 35 °C have to increase by 240%. From the formula for unstirred layer corrections it can be calculated that the contribution of the unstirred layers to the total resistance have to increase from 37% to 73%. This means an underestimation of the unstirred layers of about 100%, which is highly unlikely in view of the data of Smulders and Wright [48] on butanol diffusion through rabbit gallbladder wall. The third reason is that our apparent activation energy values for urea diffusion between 35 and 15 °C are in good agreement with values found by Smulders and Wright between 35 and 5 °C [48]. These authors stirred on both sides of the gallbladder wall. Greater unstirred layer corrections in our experiments would lead to considerably higher activation energies. For these reasons we have confidence in our statement that phloretin brings about a shift in the activation energy of urea diffusion towards higher values. The increase in antipyrine permeability, without a change in the apparent activation energy, suggests an increase in the surface available for hydrophobic interaction without a structural change in the hydrophobic region. The apparent activation energy value for antipyrine permeation is rather low compared with values for permeation through pure lipid bilayers [11]. Whatever the molecular mechanism of phloretin action on gall bladder membranes may be, the effect suggests an important role of proteins in the control of membrane nonelectrolyte permeability. Table 3 shows clearly the transition from the cellular route to another permeation possibility. From ^{3}HHO to glycerol, an enormous restriction in the diffusion is observed. This restriction is absent going from erythritol to dextran. The apparent impermeability to albumin excludes the possibility that inulin permeation is due to damaged cells or to a pinocytotic process. Pinocytotic uptake of

albumin is a well established process in renal tubules [8]. Mucosal hypertonicity induces in tight epithelia such as frog skin and toad bladder, a decrease in electrical resistance and increased sucrose fluxes [14, 52]. Changes in the zonulae occludentes are in both tissues responsible for the altered permeabilities [15, 19]. From these observations on tight epithelia and from Table 3 we conclude, therefore, that from erythritol to dextran the permeation is exclusively extracellular through the tight junction. Unobservable albumin fluxes fit well with pore radii of 40 Å in the extracellular shunt path. Another explanation could be restriction of albumin diffusion in the polysaccharide network of the connective tissue. Laurent and Öbrink [31] have demonstrated a striking effect of dextran solutions on translational diffusion of albumin without effect on the rotational movement. To exclude this possibility we studied albumin fluxes through chloroform-treated tissue in which preparation the cell membranes are destroyed [54].

P_{albumin} for $CHCl_3$-treated tissue is two orders of magnitude greater than the lowest P value which can be observed with the method used (Table 1). The $CHCl_3$ value is comparable to albumin permeability of a cell-free connective tissue preparation of toad bladder [18]. Intact toad bladder epithelium is also impermeable to albumin and in this aspect "tight" and "leaky" epithelia are not different [18]. As to how far high inulin permeabilities coupled with observable albumin fluxes (Table 2) is a normal physiological pattern or is brought about by dissection or necrosis cannot be decided.

The calculated restriction in the diffusion of dextran is more pronounced than the observed restriction. The predicted restriction is calculated with the aid of the free diffusion coefficient in Table 2. However, it has been shown that the shape of a molecule is a dominant factor for the rate of diffusion through a polymeric network [32, 42]. In free solution the diffusion rate correlates predominantly with the long dimension of an asymmetric molecule, but in a polymeric network the correlation is better with the small dimension. This means that asymmetric molecules such as inulin and dextran, with ellipticity factors of about 7, are unsuitable solutes in pore size determinations when the pores are most likely holes in a polymeric network. This type of network structure has to be expected between the cell membranes of neighboring cells at the tight junction level.

The above-mentioned phenomenon can also explain our observation that when inulin and sucrose fluxes are compared in the same bladder, the inulin flux is always greater than predicted from free-solution diffusivity and sucrose permeability. Since inulin is a rod-shaped molecule, the rate of

diffusion in the fabric of the tight junction route will correlate with the small dimension of the molecule rather than with the molecular weight.

Increasing tonicity of the incubation medium causes opposite effects on the cell membrane and the shunt pathway permeability. Water and urea permeability depend greatly on medium osmolarity. This effect is also observed in red cells [44], plant cells [10], and smooth muscle cells [29], which indicates a general osmotic behavior of biomembranes. The increase in junctional permeability with raised osmolarities may not be caused by alteration of the junctional route per se. Enlarged lateral intercellular spaces caused by cell shrinking could also be responsible [41]. Changes in the zonulae occludentes can, however, not be excluded since Bentzel [4] observed structural changes in this region in volume-expanded proximal tubules.

The most likely limiting barrier for diffusion through the shunt path is the zonula occludens facing the lumen of the bladder. In this structure the two outer leaflets of the plasma membranes are apparently fused, or the interposed intercellular space is considerably smaller than in the zonula adherens [25]. Therefore, a rough estimate of the available area for sucrose diffusion can be obtained from the sucrose permeability P_s, the free diffusivity D_s and the length l of the zonula occludens ($l = 2{,}000$ Å). This shunt area, $S_a = P_s l / D_s = 3 \times 10^{-5}$ cm^2/cm^2 epithelium.

Assuming that the surface cells of gallbladder are packed in a regular array of hexagons with side s and diameter of circumscribed circle $D = 5$ μ [51], then the area of one cell is $A = 1.5 \sqrt{3}\, s^2$. If the extracellular pathway consists of continuous slits with separation $2a = d$, and edge effects are neglected since $s \gg a$, then the area of one cell plus a half slit is $A' \sim 1.5 \sqrt{3}\, (s+a)^2$. The separation d can be obtained from $(A' - A)/A = 3 \times 10^{-5}$ which gives $d = 0.8$ Å. This means a completely impermeable tight junction area and therefore we have to think of pores instead of narrow slits.

The number of pores N with equivalent radii of 40 Å, which have been calculated from Table 3, is $N = 5 \times 10^7$ per cm^2. The number of cells per cm^2 is $n = 6 \times 10^6$. Since every pore is shared by two cells, the average distance between two pores is approximately 1 μ. This result shows that only 0.8% of the perimeter of one cell is occupied by porous structures with equivalent radii ~ 40 Å and that the vast majority of the junctional area is really tight. The possibility of dynamic pores evenly distributed over the tight junctions area cannot be excluded.

With the dimension obtained for the extracellular shunt the contribution to the osmotic flow can be evaluated. Kedem and Katchalsky [30] reported

that the mechanism of water flow through pores as small as 20 Å will be primarily laminar. Therefore we may use Poiseuille's law:

$$Q_s = N \frac{\pi r^4}{8 \eta l} \Delta P$$

where $\eta = 0.89 \times 10^{-2}$ poise (viscosity of bulk water at 20 °C), $l = 2{,}000$ Å, length of the zonula occludens, $N = 5 \times 10^{-7}$ pores per cm^2. With $\Delta P =$ 2.44 atm, equivalent to 100 mOsm liter^{-1} [38], the flow through the shunt is $Q_s = 25.6$ µliter hr^{-1} cm^{-2}.

The mean observed flow in response to 100 mOsm liter^{-1} sucrose is 32.4 µliter × hr^{-1} cm^{-2} (Table 5). If the reflection coefficient, σ_{sucrose}, is near unity in the shunt path, 80% of the osmotic flow will be through the junctions. However σ_{sucrose} can be calculated by making use of the equation derived by Goldstein and Solomon [24]:

$$1 - \sigma = \frac{[2(1-\alpha)^2 - (1-\alpha)^4][1 - 2,104\alpha + 2.09\alpha^3 - 0.95\alpha^5]}{[2(1-\beta)^2 - (1-\beta)^4][1 - 2,104\beta + 2.09\beta^3 - 0.95\beta^5]}$$

where $\alpha = R_s/R_p$ is the ratio of solute radius to pore radius and $\beta = R_w/R_p$ is the ratio of water radius to pore radius. Inserting $R_w = 1.5$ Å, $R_s = 5$ Å and $R_p = 40$ Å leads to $\sigma_{\text{sucrose}} = 0.2$. Durbin [17] determined $\sigma_{\text{sucrose}} = 0.07$ for cellophane membranes with equivalent radii of 41 Å. Taking these two σ values, the contribution of the shunt to the osmotic flow is between 6 and 16% of the total flow. Thus, osmotic flow induced by sucrose is passing mainly through the cell membranes, a conclusion in agreement with earlier reports [54, 57].

During active reabsorption the osmotic gradient is built up by actively transported NaCl. In this situation we need detailed information about σ_{NaCl} for the lateral cell membranes and for the junctional route. Table 5 shows that the osmotic efficiency of NaCl is smaller than that of sucrose. Since the lateral cell membranes are the site of active Na^+ transport, which implies a σ_{NaCl} of about unity, the shunt contribution during active reabsorption will be less than 16%. Greater osmotic fluxes are observed for TEACl and albumin compared to identical osmotic gradients of sucrose. This suggests greater σ values for the shunt pathway. $\sigma_{\text{albumin}} = 0.999$, as calculated from Goldstein and Solomon's equation, using $R_{\text{albumin}} = 37$ Å and $R_{\text{pore}} = 40$ Å.

However, the small water flux measurements with 20% albumin Ringer's solutions are subject to great experimental error. The increase in water

flux compared with 20 mOsm × liter^{-1} sucrose ranged from 0 to 200%. 20% (w/v) albumin added to Ringer's solution raises the osmolarity by 20 mOsm. The same rise in osmolarity is observed for 20% albumin in distilled water. This implies an osmotic coefficient for albumin of about 5, which is rather high. Dick [16] reported, for a 10% albumin solution, an osmotic coefficient of 2.45. Although the small water fluxes in response to 20 mOsm and the osmotic coefficient of albumin are complicating factors, Schnermann, Agerup and Persson [45] have shown that albumin is also osmotically more effective in rat proximal tubules than raffinose.

The conclusion can be drawn that the extracellular shunt pathway does not contribute significantly to the osmotic water flow during active reabsorption. The primary role of this shunt must be sought in the equivalent electrical circuit, since a low resistance shunt has drastic effects on the transcellular potential difference and on the cellular potential.

References

1. Altamirano, M., Martinoya, C. 1966. The permeability of the gastric mucosa of dog. *J. Physiol.* **184**:771
2. Barry, P. H., Diamond, J. M., Wright, E. M. 1971. The mechanism of cation permeation in rabbit gallbladder. Dilution potentials and biionic potentials. *J. Membrane Biol.* **4**:358
3. Beck, R. E., Schultz, J. S. 1972. Hindrance of solute diffusion within membranes as measured with microporous membranes of known pore geometry. *Biochim. Biophys. Acta* **255**:273
4. Bentzel, C. J. 1972. Proximale tubule structure-function relationships during volume expansion in *Necturus*. *Kidney International* 2:324
5. Bentzel, C. J., Davies, M., Scott, W. N., Zatzman, M., Solomon, A. K. 1968. Osmotic volume flow in the proximal tubule of *Necturus* kidney. *J. Gen. Physiol.* **51**:517
6. Blum, A. L., Hirschowitz, B. I., Helander, H. F., Sachs, G. 1971. Electrical properties of isolated cells of *Necturus* gastric mucosa. *Biochim. Biophys. Acta* **241**:261
7. Boulpaep, E. L. 1967. Ion permeability of the peritubular and luminal membrane of the renal tubular cell. *In*: Transport und Function intracellulärer Elektrolyte. F. Krück, editor. p. 98. Urban und Schwarzenberg, München, Germany
8. Bourdeau, J. E., Carone, F. A., Ganote, C. E. 1972. Serum albumin uptake in isolated perfused renal tubules: Quantitative and electron microscope radioautographic studies in three anatomical segments of the rabbit nephron. *J. Cell Biol.* **54**:382
9. Bray, G. 1960. Simple efficient liquid scintillator for counting aqueous solution in a liquid scintillation counter. *Analyt. Biochem.* **1**:279
10. Dainty, J., Ginzburg, B. Z. 1964. The permeability of the cell membranes of *Nitella translucens* to urea and the effect of high concentrations of sucrose on this permeability. *Biochim. Biophys. Acta* **79**:112

11. De Gier, J., Mandersloot, J. G., Hupkes, J. V., McElhaney, R. N., Van Beek, W. P. 1971. On the mechanism of non-electrolyte permeation through lipid bilayers and through biomembranes. *Biochim. Biophys. Acta* **233**:610
12. Diamond, J. M. 1964. Transport of salt and water in rabbit and guinea pig gallbladder. *J. Gen. Physiol.* **48**:1
13. Diamond, J. M., Wright, E. M. 1969. Molecular forces governing non-electrolyte permeation through cell membranes. *Proc. Roy. Soc. (London) B.* **172**:273
14. DiBona, D. R. 1972. Passive intercellular pathway in amphibian epithelia. *Nature, New Biol.* **238**:179
15. DiBona, D. R., Civan, M. M. 1973. Pathways for movement of ions and water across toad urinary bladder. *J. Membrane Biol.* **12**:101
16. Dick, D. A. T. 1959. Osmotic properties of living cells. *Int. Rev. Cytol.* **8**:387
17. Durbin, R. P. 1960. Osmotic flow of water across permeable cellulose membranes. *J. Gen. Physiol.* **44**:315
18. Elsbach, P., Pettis, P. 1972. A connective tissue membrane as a molecular sieve. *Biochim. Biophys. Acta* **255**:149
19. Erlij, D., Martinez-Palomo, A. 1972. Opening of tight junctions in frog skin by hypertonic urea solutions. *J. Membrane Biol.* **9**:229
20. Franki, N., Levine, S., Hays, R. M. 1972. Evidence that vasopressin opens independent pathways for water and urea in the cell membrane. *Proc. 5th Int. Congr. Nephrology.* p. 78 (abstr.)
21. Frizzell, R. A., Schultz, S. G. 1972. Ionic conductances of extracellular shunt pathway in rabbit ileum. *J. Gen. Physiol.* **59**:318
22. Frömter, E. 1972. The route of passive ion movement through the epithelium of *Necturus* gallbladder. *J. Membrane Biol.* **8**:259
23. Gertz, K. H. 1963. Transtubuläre Natriumchloridflüsse und Permeabilität für Nichtelektrolyte in proximalen und distalen Konvolut der Rattenniere. *Pflüg. Arch. Ges. Physiol.* **276**:336
24. Goldstein, D. A., Solomon, A. K. 1960. Determination of equivalent pore radius for human red cells by osmotic pressure measurements. *J. Gen. Physiol.* **44**:1
25. Goodenough, D. A., Revel, J. P. 1970. A fine structural analysis of intercellular junctions in the mouse liver. *J. Cell Biol.* **45**:272
26. Hingson, D. J., Diamond, J. M. 1972. Comparison of nonelectrolyte permeability patterns in several epithelia. *J. Membrane Biol.* **10**:93
27. Holtz, R., Finkelstein, A. 1970. The water and non-electrolyte permeability induced in thin lipid membranes by the polyene antibiotics Nystatin and Amphotericin B. *J. Gen. Physiol.* **56**:125
28. International Critical Tables, 1929. Vol. V, p. 63. McGraw-Hill, New York
29. Jonsson, O. 1971. Effect of variations in the extracellular osmolarity on the permeability to nonelectrolytes of vascular smooth muscle. *Acta Physiol. Scand.* **81**:528
30. Kedem, O., Katchalsky, A. 1961. A physical interpretation of the phenomenological coefficients of membrane permeability. *J. Gen. Physiol.* **45**:143
31. Laurent, T. C., Öbrink, B. 1972. On the restriction of rotational diffusion of proteins in polymer networks. *Europ. J. Biochem.* **28**:94
32. Lieb, W. R., Stein, W. D. 1971. Implications of two different types of diffusion for biological membranes. *Nature, New Biol.* **234**:220
33. Loehry, C. A., Axon, A. T. R., Hilton, P. J., Hider, R. C., Creamer, B. 1970. Permeability of the small intestine to substance of different molecular weight. *Gut* **11**:466

34. Longsworth, L. G. 1953. Diffusion measurements, at 25 °C, of aqueous solutions of amino acids, peptides and sugars. *J. Clin. Chem. Soc.* **75**:5705

35. Longsworth, L. G. 1954. Temperature dependence of diffusion in aqueous solutions. *J. Phys. Chem.* **58**:770

36. Lyons, P. A., Sandquist, C. L. 1953. A study of the diffusion of *n* butyl alcohol in water using the Gouy method. *J. Amer. Chem. Soc.* **75**:3896

37. Macey, R. I., Farmer, R. E. L. 1970. Inhibition of water and solute permeability in human red cells. *Biochim. Biophys. Acta* **211**:104

38. Mauro, A. 1965. Osmotic flow in a rigid porous membrane. *Science* **149**:867

39. Ogston, A. G., Woods, E. F. 1954. The sedimentation of some fractions of degraded dextran. *Trans. Faraday Soc.* **50**:635

40. Owen, J. D., Solomon, A. K. 1972. Control of nonelectrolyte permeability in red cells. *Biochim. Biophys. Acta* **290**:414

41. Phelps, C. F. 1965. The physical properties of inulin solutions. *Biochem. J.* **95**:41

42. Preston, B. N. 1972. Diffusion properties of model extracellular systems. *Juselius Symp.* "Biology of the fibroblast" (Turku)

43. Renkin, E. M. 1955. Filtration, diffusion and molecular sieving through porous cellulose membranes. *J. Gen. Physiol.* **38**:225

44. Rich, G. T., Sha'afi, R. I., Romaldez, A., Solomon, A. K. 1968. Effect of osmolarity on the hydraulic permeability coefficient of red cells. *J. Gen. Physiol.* **52**:941

45. Schnermann, J., Agerup, B., Persson, E. 1972. Hydraulic conductivity of proximal tubules in the rat kidney as determined by colloid osmotically induced water fluxes. *Pflüg. Arch. Ges. Physiol.* **332**s:63

46. Schultz, S. G., Solomon, A. K. 1961. Determination of the effective hydronamic radii of small molecules by viscometry. *J. Gen. Physiol.* **44**:1189

47. Smulders, A. P., Tormey, J. McD., Wright, E. M. 1972. The effect of osmotically induced water flows on the permeability and ultrastructure of the rabbit gallbladder. *J. Membrane Biol.* **7**:164

48. Smulders, A. P., Wright, E. M. 1971. The magnitude of nonelectrolyte selectivity in the gallbladder epithelium. *J. Membrane Biol.* **5**:297

49. Soll, A. H. 1967. A new approach to molecular configuration applied to aqueous pore transport. *J. Gen. Physiol.* **50**:2565

50. Stein, W. D. 1967. The movement of molecules across cell membranes. Academic Press Inc., New York-London

51. Tormey, J. McD., Diamond, J. M. 1967. The ultrastructural route of fluid transport in rabbit gallbladder. *J. Gen. Physiol.* **50**:2032

52. Ussing, H. H. 1966. Anomalous transport of electrolytes and sucrose through the isolated frog skin induced by hypertonicity of the outside bathing solution. *Ann. N. Y. Acad. Sci.* **137**:543

53. van Os, C. H., Slegers, J. F. G. 1971. Correlation between (Na^+-K^+)-activated ATPase activities and the rate of isotonic fluid transport of gallbladder epithelium. *Biochim. Biophys. Acta* **241**:89

54. van Os, C. H., Slegers, J. F. G. 1973. Path of osmotic water flow through rabbit gall bladder epithelium. *Biochim. Biophys. Acta* **291**:197

55. Wand, J. W., Robinson, C. V., Edelman, J. S. J. 1953. Self diffusion and structure of liquid water. III. Measurements of the self diffusion of liquid water with H^2, H^3 and O^{18} as tracers. *J. Amer. Chem. Soc.* **75**:466

56. Wright, E. M., Diamond, J. M. 1969. Patterns of non-electrolyte permeability. *Proc. Roy. Soc. (London) B.* **172**:227

57. Wright, E. M., Smulders, A. P., Tormey, J. McD. 1972. The role of the lateral intercellular spaces and solute polarization effects in the passive flow of water across the rabbit gallbladder. *J. Membrane Biol.* **7**:198